Deep space reception of Tianwen-1 by AMSAT-DL using GNU Radio

Daniel Estévez DANIEL@DESTEVEZ.NET

Mario Lorenz DL5MLO@AMSAT-DL.ORG

Peter Gülzow DB2OS@AMSAT-DL.ORG

Abstract

This paper describes the reception of the Tianwen-1 Chinese Mars mission carried out by AMSAT-DL with the 20 meter antenna at Bochum Observatory (Germany). A real-time GNU Radio decoder has been used to receive and store telemetry almost every day over the course of 10 months. Some of the telemetry variables, such as the trajectory information, have been successfully interpreted and used to track the progress of the mission.

1. Introduction

Tianwen-1 is a Chinese mission to Mars that consists of a rover called Zhurong and an orbiter spacecraft (Wan et al., 2020). The rover is currently studying the geological and topographical properties of its landing site in Utopia Planitia (Wu et al., 2021; Wang et al., 2021a), including the search for water ice in the soil (Wang et al., 2021b), while the orbiter is surveying the topography of Mars as well as other geophysical properties such as the ionosphere and the magnetic field (Zou et al., 2021). The orbiter also serves as a communications relay for the rover.

The spacecraft launched on 23 July 2020 from Hainan. This mission triggered some interest in the amateur spacecraft tracking and amateur radio communities, because the spacecraft frequency allocations and orbital information were not publicly available. For missions from other agencies, the frequencies used are often well-known and trajectory information is available from NASA HORIZONS. Without this data, Tianwen-1 provided an interesting challenge.

Amateurs from Europe were able to detect the spacecraft a few hours after launch using spectrum analyzers and small low-gain X-band horn antennas. They also performed some IQ recordings with SDR devices for later analysis. The X-band telemetry from these recordings could be decoded with GNU Radio (see Section 3), and it was possible to interpret some of the telemetry data, including the spacecraft's trajectory information (see Section 4).

The availability of orbit information directly decoded from the spacecraft allowed for its position on the sky to be computed with precision. This permitted amateur operators from AMSAT-DL to use the 20 meter antenna at Bochum Observatory to find and track Tianwen-1 a few days after launch (see Section 2). At X-band this antenna has a beamwidth of only 0.1 degrees.

Since then, AMSAT-DL has been tracking Tianwen-1 with Bochum Observatory almost every day, and using a real-time GNU Radio decoder to receive and store the spacecraft's telemetry. AMSAT-DL has followed Tianwen-1 through all the major events in the mission, including maneuvers on the coast from Earth to Mars, the orbital insertion at Mars, subsequent orbit changes, and the release of the Zhurong rover and lander (see Section 6). Additionally, a YouTube livestream has been used for public outreach, showing the spectrum and waterfall of the signals received during some events (see Section 5).

Over a period of 313 days, a total of around $5.9 \cdot 10^9$ bytes of telemetry data have been received. At a rate of 7040 bps, this represents around 232 hours of successful telemetry reception. As of writing this paper, at the beginning of September 2021, Bochum Observartory is still decoding successfully signals from Tianwen-1 at a distance of 393 million km. This distance keeps increasing every day, and is already quite close to the maximum distance between Earth and Mars, which is 401 million km. To our knowledge, this constitutes a record of the farthest digital communication being decoded in real-time with GNU Radio.

2. Bochum Observatory and AMSAT-DL

The 20 meter parabolic antenna of Bochum Observatory was built under a radome and inaugurated in November 1967 after a construction time of almost 3 years. Bochum Observatory was well known back then for having been the first western station to confirm Sputnik 1 signals in 1957.

Over the years, many near-earth, moon and deep space missions were tracked, like the Luna series including Lunachod 1 and Pioneer 8 (Kaminski, 1976). The reception and recording of voice, telemetry and image transmissions of the US APOLLO 11 and later Moon missions were a special highlight in the history of the antenna and the observatory (Kaminski, 1972).

At the end of the 1990s the antenna was no longer operational and its radome ruptured. A complete technical overhaul was begun. All antenna pointing control and drive systems, as well as the receiving equipment, were fundamentally redeveloped and rebuilt. This enabled the required pointing accuracy for X-Band work.

Since then, the station has been run by a group of volunteers of AMSAT-DL together with the Observatory staff, and its facilities were continuously improved. The reception capabilities of the antenna were demonstrated by the tracking of Voyager-1 in March 2006, at a distance of over 98AU.

The background to AMSAT-DL's involvement was the AMSAT P5-A project to launch its own Mars mission in collaboration with DLR and to use the 20 meter antenna in Bochum as a ground station (Quantius & Romberg, 2010; Quantius et al., 2010). In 2011-2012 a feasibility study was successfully conducted. Nevertheless the project was unfortunately put on hold in 2013.

In 2009, AMSAT-DL also succeeded in producing and receiving echoes at Venus using the high-power magnetron transmitter (5kW power on 2.4GHz) it developed for that purpose.

The main task of the 20 meter antenna since 2009 is the reception of the STEREO-A/B spacecraft on a daily basis, forwarding the real-time Space Weather Beacon data to the NASA/NOAA for further analysis (Ratti et al., 2013). The station has been used in other projects as opportunities arose, for example for the ISEE-3 reboot (Dunham et al., 2015).

In the meantime, many more deep space probes have been tracked. Next to interplanetary probes like New Horizons, Rosetta, Ulysses and Venus Climate Orbiter, the list includes practically all space probes in Mars orbit, in particular the most recently launched spacecraft EMM (Hope Mars Mission) and Mars 2020.

At X-Band, the dish has a gain of 62.5dBi, and a T_{sys} of about 150K, mainly limited by the radome.

As shown in Figure 1, the receive signal from the RHCP/LHCP X-Band feed is preamplified using a Kuhne KU LNA 8000A and then downconverted to a 1.2GHz IF. The signal is then split. An AOR-5000A is used for general narrowband reception, whereas an USRP N210 is available

for wideband work and SDR based data decoding. Finally, an AirSpy connected to a Windows workstation running SDRSharp provided visualization and streaming.
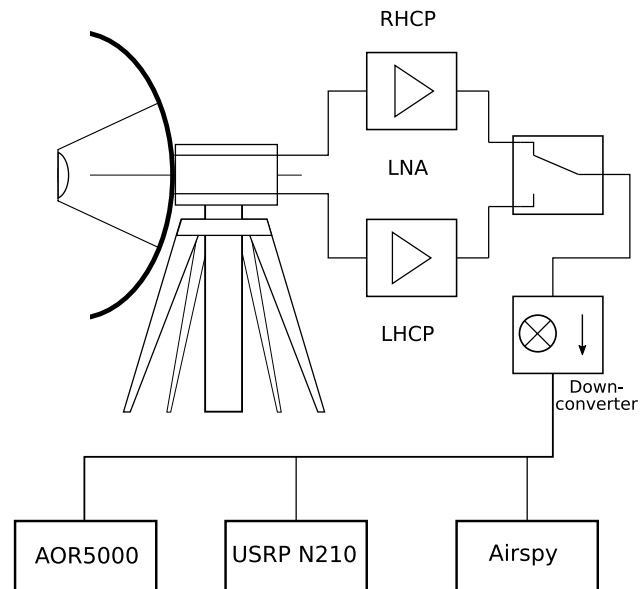
Figure 1. Bochum Observatory X-Band reception setup)

All devices are reference-locked to a 10MHz GPS disciplined reference oscillator.

3. GNU Radio decoder

The modulation and coding used by Tianwen-1 was first reverse-engineered in (r00t.cz, 2020), and then independently in (Estévez, 2020a). Its parameters are summarized in Table 1. The *low rate* column refers to the low rate telemetry used most of the time to transmit real-time telemetry. The *high speed* column refers to a high speed signal that was occasionally used to replay recorded telemetry or transmit payload data. The configuration shown for the high speed signal refers to the one used at the beginning of the mission, during the coast from Earth to Mars. A lower rate variant of the high speed signal was observed later in the mission, around May 2021, when Mars was much further, at 300 million km from Earth.

The main activity of Bochum observatory regarding the Tianwen-1 mission consisted in the real-time decoding of the low rate signal using GNU Radio. A decoder for the high speed signal was also implemented and tested with IQ recordings. Unfortunately, we were not able to demonstrate the real-time decoding capability of the high speed decoder at Bochum, due to CPU constraints in the PC of the observatory (which prevented both the low rate and high speed decoder from running simultaneously) and to the un-

	Low rate	High speed
Carrier	8431 MHz	8431 MHz
Modulation	PCM/PSK/PM	QPSK
Baudrate	16384 baud	2.048 Mbaud
Subcarrier	65536 Hz	—
Convolutional	$r = 1/2, k = 7$	$r = 1/2, k = 7$
Reed-Solomon	(252, 220)	4x (255, 223)
Link layer	CCSDS AOS	CCSDS AOS
Network layer	CCSDS/ad-hoc	CCSDS/ad-hoc

Table 1. Tianwen-1 modulation and coding

predictability of the high speed transmission sessions.

3.1. Low rate decoder

The low rate signal of Tianwen-1 is a residual-carrier phase-modulated signal with the data BPSK-modulated onto a square wave subcarrier. The decoder uses the techniques presented in a workshop in GRCon20 (Estévez, 2020b). Figure 2 shows the first part of the decoder flowgraph. First, a PLL is used to lock to the residual carrier, and the phase modulation is extracted from the quadrature part of the signal. Then the data sideband, which is present in a BPSK-modulated subcarrier at 65.536 kHz, is moved to baseband. A coarse pulse-shape filter is implemented by a moving average.
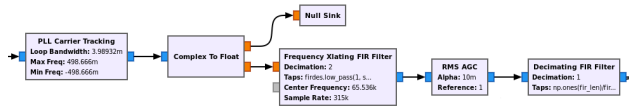
Figure 2. Tianwen-1 low rate decoder flowgraph (first section)

The remaining part of the decoder is shown in Figure 3. The Symbol Sync block (Walls, 2017) with a Gardner TED is used for symbol clock recovery. A Costas loop (Costas, 1956) removes the phase offset and drift between the actual subcarrier signal and the nominal subcarrier used in the downconversion described above. It is interesting to remark that even though there were exactly 4 subcarrier cycles per BPSK symbol, it appears that the subcarrier and BPSK symbols were clocked independently on the spacecraft. This made the subcarrier and symbol clocks drift with respect to each other, causing periodic changes in the power spectral density of the signal.

The BPSK modulation is extracted from the real part of the signal. Finally, the CCSDS Concatenated Deframer block from gr-satellites (Estévez, 2016) is used to perform Viterbi decoding, detect the ASM (Attached Sync Marker) that indicates the beginning of the Reed-Solomon codewords, perform descrambling, and Reed-Solomon decoding. At

the output of this block, PDUs containing 220 byte CCSDS AOS Space Data Link frames (CCSDS AOS) are obtained.

Two copies in parallel of the CCSDS Concatenated Deframer are used due to the 180° phase ambiguity of the Costas loop. One of the copies receives the symbol stream and the other copy receives the inverted symbol stream, so that one of the two will get the correct symbols.
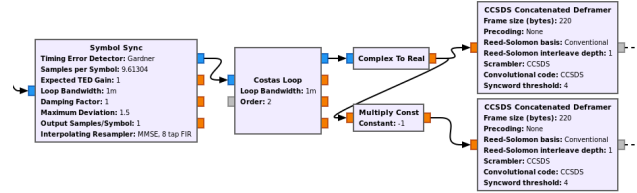
Figure 3. Tianwen-1 low rate decoder flowgraph (second section)

3.2. High speed decoder

The differences between the high speed signal and the low rate signal are the use of a suppressed-carrier QPSK modulation instead of the residual-carrier phase modulation, and that often a larger frame size consisting of 4 interleaved Reed-Solomon (255, 223) codewords is employed (although the same frame size as in the low rate signal is also possible). Additionally, the convolutional coding of the high speed signal does not follow the CCSDS Blue Book (CCSDS TM) exactly, since the inverter in one of the branches of the encoder is missing, unlike in the case of the low rate signal.

The structure of the high speed decoder is quite similar to that of the low rate decoder. The main differences are in the demodulation and the handling of the phase ambiguity. The first part of the flowgraph, shown in Figure 4, is a simple QPSK demodulator. It uses the Symbol Sync block for polyphase RRC filtering with a maximum likelyhood TED, and a Costas loop for carrier phase recovery.
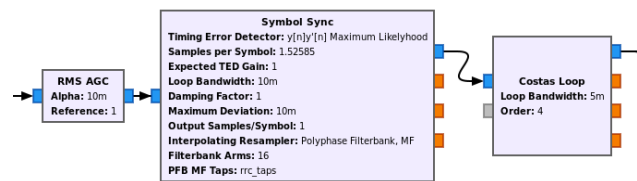
Figure 4. Tianwen-1 high rate decoder flowgraph (first section)

The next section, which can be found in Figure 5 performs Viterbi decoding using the FEC Extender Decoder block. Since the Costas loop has a phase ambiguity of 90° (or any integer multiple of this), it is necessary to try Viterbi decod-

ing on the stream of symbols and the stream of symbols rotated 90º. This still leaves the possibility of an uncorrected 180º phase rotation. However, we exploit the property that the CCSDS convolutional code commutes with the inversion (the same result is obtained if the input or the output of the convolutional encoder are inverted) to defer the handling of the 180º phase rotation to a later stage.
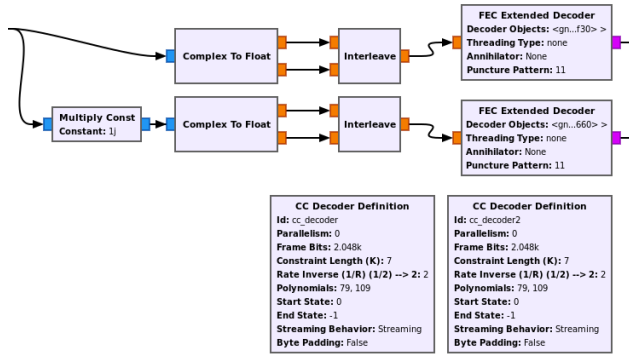
Figure 5. Tianwen-1 high speed decoder flowgraph (second section)

The final section of the decoder, shown in Figure 6 takes into account the possible 180º phase rotation and uses the Sync and create PDU block from gr-satellites to detect the ASMs and extract PDUs of the appropriate size from the symbol stream. These PDUs are descrambled and Reed-Solomon decoded using blocks from gr-satellites.
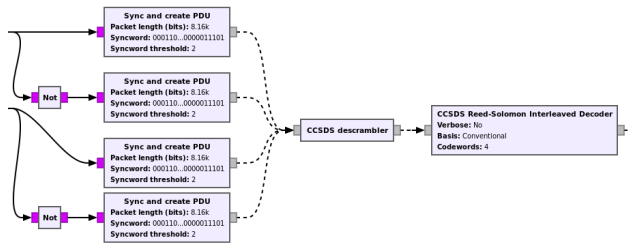
Figure 6. Tianwen-1 high speed decoder flowgraph (third section)

4. Telemetry decoding

Part of the telemetry of Tianwen-1 was reverse-engineered by r00t.cz, using his own decoder, and by Estévez, using the GNU Radio decoder presented here. Many telemetry channels that show interesting patterns were identified, but a satisfactory interpretation has only been found for a few of them.

Tianwen-1 uses CCSDS AOS Space Data Link frames. In most cases, these frames contain fragmented CCSDS Space Packets (CCSDS Space Packet), although in some cases ad-hoc framing is used. The low data rate telemetry signal uses the following SCID (spacecraft identifier) and VCID (virtual channel identifier) combinations:

- SCID 245 VCID 1. This is used for real-time telemetry and contains several dozens of different Space Packet APIDs.

- SCID 245 VCID 2. Is used very seldom and contains only a few different Space Packet APIDs. Details about the kind of data in this VCID are not known.

- SCID 245 VCID 3. Only contains padding.

- SCID 84 VCID 1. Contains data from the lander stage, using Space Packets with several different APIDs. During the coast from Earth to Mars it displayed mostly unchanging data. After separation of the lander stage on 14 May 2021, this channel disappeared from the telemetry. Analysis of this channel in the telemetry recorded at Bochum during EDL (entry, descent and landing) showed relayed information from the lander through the orbiter during the descent (as evidenced by the replay flag in the AOS frames). Bochum has not been able to receive relayed information from the lander afterwards, since the relay sessions are rather sporadic.

A small number of high speed data communication sessions recorded by radio amateurs have also been analyzed. Besides the VCIDs listed above, it is also noteworthy APID 24, which uses a custom framing to send several months worth of recorded telemetry data.

4.1. State vectors

Probably the most interesting contents in the telemetry are the state vectors. These contain the timestamped position and velocity vectors of the spacecraft, allowing us to propagate the spacecraft trajectory. The presence of a series of double-precision IEEE 754 floating point numbers in the telemetry was noticed by r00t.cz, and Estévez was able to identify that these were state vectors on the same day that Tianwen-1 was launched.

The state vectors are transmitted in APID 1287 in SCID 245 VCID 1. They are composed of a 48 bit timestamp, which gives the number of 100 μs units elapsed since 2015-12-31 16:00:00 UTC (which is 2016-01-01 00:00:00 Beijing time), the position vector, given as three doubles in km units, and the velocity vector, given as three doubles in km/s units.

During the coast from Earth to Mars, the reference system for the state vectors was heliocentric MJ2000 or ICRF coordinates (due to the small difference between these two

systems (Kaplan, 2005), it has not been possible to tell which was used). Between 7 and 8 February 2021, when the spacecraft was arriving at Mars, the coordinate system changed to Mars centric body inertial coordinates. In this system, the z-axis points along the spin axis of Mars at the J2000 epoch, the x-axis points along the intersection of the xy-plane of the FK5 system at the J2000 epoch and the plane orthogonal to the spin axis, and the y-axis completes the right-handed orthonormal system.

4.2. ADCS telemetry

Another part of the telemetry which has been successfully explained is the ADCS (attitude determination and control system). This was reverse-engineered with the help of the telemetry collected during an attitude change maneuver executed on 29 July 2020. This telemetry was replayed by the spacecraft over high speed data shortly afterwards. After analysis, it was determined that the maneuver had consisted in a -15° rotation about the y-axis, which provided a very simple scenario to exercise all the ADCS telemetry channels.

This telemetry is transmitted in APIDs 1280, 1281 and 1282 in SCID 245 VCID 1. It contains the following variables:

- Angular errors and angular rate errors from the attitude controler

- Angular rates measured by three sets of redundant gyroscopes; one of the sets seems to have lower quality

- Attitude quaternions encoding the body-frame to ICRF-frame rotation

Additionally, there are other variables that show similar patterns. We have not been able to explain these, but it is possible that some contain reaction wheel data.

Figure 7 shows some of the ADCS telemetry variables during the -15° rotation maneuver. The upper left quadrant shows the controller errors of the y-axis. The maneuver starts with a 15° angular error introduced in the controller. As the spacecraft starts rotating, the angular rate error becomes nonzero, but the angular error decreases. The lower left quadrant shows one of the y-axis gyroscope measurements. It gives a noisier version of the angular rate error. The scale in these two plots is arbitrary, but the zero level is shown. The x and z-axis data is not shown, since it is very close to zero, as the maneuver does not involve these axes.

The upper left quadrant shows the attitude quaternions, appropriately scaled to unit norm (they are transmitted as 16 bit integers with a scaling factor of 10000). Finally, the lower right quadrant shows the rotation angle about the

y-axis, relative to the start of the maneuver. This is not transmitted in the telemetry directly, but computed from the quaternion data.
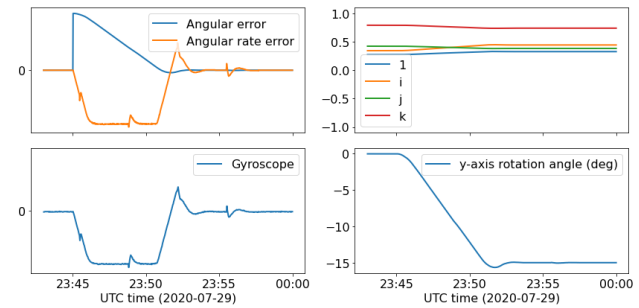
Figure 7. ADCS telemetry during -15° rotation about y-axis

The spacecraft body frame is defined by the y-axis pointing along the solar panels, the x-axis pointing in the direction opposite to the thrust vector of the main thrusters, and the z-axis pointing roughly opposite to the high-gain antenna. This was deduced from the study of the spacecraft attitude during its Earth-Mars cruise and confirmed with an image from the control center that appeared in social media (see Figure 8).
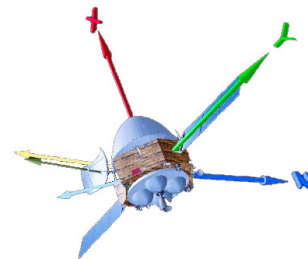
Figure 8. Tianwen-1 spacecraft body axes

The nominal attitude during both Earth-Mars cruise and Mars orbit was with the y-axis orthogonal to the ecliptic plane, and a fixed angle between the sun vector and the x-axis. This angle was changed a couple times during the mission, perhaps for thermal management reasons. One of those changes is the -15° rotation maneuver described above.

The attitude only deviates from nominal during maneuvers. In these cases, the high-gain antenna is not aimed towards Earth, so Bochum cannot decode telemetry, due to the much lower signal power. The real-time data recorded during the maneuver is typically replayed over high speed data after the maneuver has finished. However, due to the difficulties decoding high speed data, we have not been able

to receive the ADCS data for any of the maneuvers, besides the one depicted above.

5. AMSAT-DL livestream

During important maneuvers, like the arrival at Mars or the separation of the lander, the Bochum team live-streamed the reception of signals from Tianwen-1 on AMSAT-DL's Youtube channel (AMSAT-DL e.V., 2021) for public outreach.

An auxillary SDR (Airspy) was added to the usual X-Band reception setup in Bochum to be able to present such data without any interference of the data decoder. The screen, displaying the RF spectrum as received, was then captured and fed to Youtube. Depending on the currently active antenna at the probe and the orientation of the spacecraft, only the residual carrier was visible, some times not even that. Nevertheless, this "engineering view" was met with considerable interest by a world wide audience consisting of lay people, enthusiasts and experts alike.

The received comments and feedback show that there is a general interest also in technical reporting, as opposed to the general, typically PR-driven shows that are usually run for major astronautic events like rocket launches.

We therefore consider the capability to make and share such observations an important educational tool to show the real work of space communications engineering and radiometric spacecraft tracking.

In the grand picture of a successful mission to another planet, these are a minor, albeit very important, detail.

6. Tracking the mission progress

The state vector data decoded from Tianwen-1's telemetry (see Section 4.1) has given us a complete account of the spacecraft's trajectory, since the data can be propagated in time to fill in gaps where telemetry was not received. We used this data to track the mission progress, observing how the maneuvers had been executed, trying to predict how future maneuvers would be done, and comparing our data with reports from official sources.

The propagation of the state vectors was performed with GMAT, an open source space mission design and simulation tool developed by NASA and industry (Thinking Systems, Inc., 2020). GMAT implements several numerical integrators and accurate force models that simulate n-body forces, non-spherical gravity, solar radiation pressure and relativistic effects.

Figure 9 shows a GMAT simulation of the Mars orbit insertion. The orbit is seen from Mars north pole. The spacecraft arrives in a hyperbolic orbit, performs a retrograde burn around periapsis, and enters a highly elliptical orbit. The burn is simulated accurately using the spacecraft's propulsion characteristics and the burn duration stated by official sources.
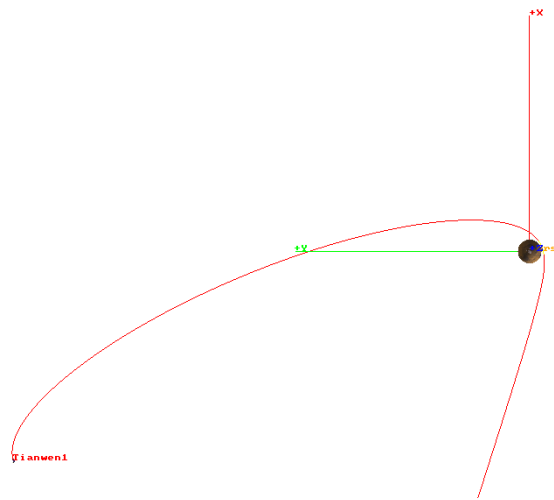
Figure 9. Tianwen-1 Mars orbit insertion simulated in GMAT

Between launch and June 2021, Tianwen-1 has performed the following orbital maneuvers according to our study of the mission.

- Trajectory correction maneuvers (TCM) during the coast from Earth to Mars:
    - 1 August 2020, TCM-1, $\Delta v \approx 14.9 \, \mathrm{m/s}$
    - 20 September 2020, TCM-2, $\Delta v \approx 4.3 \, \mathrm{m/s}$
    - 9 October 2020, Deep Space Maneuver, $\Delta v \approx 312 \, \mathrm{m/s}$
    - 28 October 2020, TCM-3, $\Delta v \approx 2.1 \, \mathrm{m/s}$
    - 5 February 2021, TCM-4, $\Delta v \approx 0.6 \, \mathrm{m/s}$

- 10 February 2021, Mars orbit injection, into a $390 \times 182000 \, \mathrm{km}$, 11° inclination orbit, $\Delta v \approx 660 \, \mathrm{m/s}$

- 15 February 2021, plane change maneuver into an 87° inclination orbit at the first apoapsis of the capture orbit, $\Delta v \approx 128 \, \mathrm{m/s}$

- 20 February 2021, apoapsis lowering to phase with the landing location longitude; change into a $280 \times 84600 \, \mathrm{km}$ orbit, $\Delta v \approx 53 \, \mathrm{m/s}$

- 23 February 2021, apoapsis lowering to change into a 2 Mars sidereal day orbit that always passes over the landing site, $\Delta v \approx 41 \, \mathrm{m/s}$

- At least 4 small maneuvers to maintain the 2 Mars sidereal day orbit

- 14 May 2021, maneuvers for the landing of Zhurong:

  - Deorbit burn, $\Delta v \approx 21 \, \mathrm{m/s}$
  - Release of the lander
  - Collision avoidance burn by the orbiter, sending it back into a 2 Mars sidereal day orbit, $\Delta v \approx 61 \, \mathrm{m/s}$

- 17 May 2021, change into a 1/3 Mars sideral day orbit intended for communications relay with the rover

- Some small maneuvers to maintain the 1/3 Mars sidereal day orbit

The Δv values shown above were obtained from a comparison of the pre-burn and post-burn trajectories. By finding their intersection, the time of the burn and Δv vector can be computed. The values should be considered approximate, since we do not know the accuracy of the state vectors, specially after a maneuver, when the spacecraft seems to transmit a pre-programmed path until the actual effects of the burn are determined by the Chinese DSN and uplinked to the spacecraft's on-board computer.

During the mission we compared these Δv values with the burn durations stated by official sources, taking into account the force and exhaust velocity of the engines. The main thrusters had a force of $3 \, \mathrm{kN}$ and exhaust velocity of $3150 \, \mathrm{m/s}$. This served as a cross-check of our data and allowed us to keep a rough fuel usage tally.

By taking into account the mission goals and some optimization constraints (such as minimizing the Δv spent), we were able to predict when some of these maneuvers would happen. Official sources only announced the burns with short notice or a posteriori, so this knowledge allowed us to focus our attention and observing time on important events and to set up public livestreams.

For instance, we could deduce that the plane change burn should happen at the first apoapsis of the capture orbit, in order to minimize the Δv cost. The condition that the 2 Mars sidereal day orbit had a repeating groundtrack whose periapsis passed over the landing location also gave useful constraints to some of the maneuvers, such as the phasing burn.

Software

The GNU Radio flowgraphs used to decode Tianwen-1 can be found in the following repository:
https://github.com/daniestevez/grcon-tianwen-paper

Acknowledgments

References

AMSAT-DL e.V. AMSAT-DL Youtube channel, 2021. URL https://youtube.com/user/amsatdl.

CCSDS AOS. AOS Space Data Link Protocol. ser. Blue Book, No. 3, September 2015. URL https://public.ccsds.org/Pubs/732x0b3e1.pdf.

CCSDS Space Packet. Space Packet Protocol. ser. Blue Book, No. 2, June 2020. URL https://public.ccsds.org/Pubs/133x0b2e1.pdf.

CCSDS TM. TM Synchronization and Channel Coding. ser. Blue Book, No. 3, September 2017. URL https://public.ccsds.org/Pubs/131x0b3e1.pdf.

Costas, John P. Synchronous communications. *Proceedings of the IRE*, 44(12):1713–1718, 1956. doi: 10.1109/JRPROC.1956.275063.

Dunham, David W., Farquhar, Robert W., Loucks, Michel, Roberts, Craig E., Wingo, Dennis, Cowing, Keith L., Garcia, Leonard N., Craychee, Tim, Nickel, Craig, Ford, Anthony, Colleluori, Marco, Folta, David C., Giorgini, Jon D., Nace, Edward, Spohr, John E., Dove, William, Mogk, Nathan, Furfaro, Roberto, and Martin, Warren L. The 2014 earth return of the ISEE-3/ICE spacecraft. *Acta Astronautica*, 110:29–42, 2015. ISSN 00945765. doi: 10.1016/j.actaastro.2015.01.002. URL https://linkinghub.elsevier.com/retrieve/pii/S0094576515000053.

Estévez, Daniel. gr-satellites, 2016. URL https://github.com/daniestevez/gr-satellites.

Estévez, Daniel. Tianwen-1 telemetry: modulation and coding, 2020a. URL https://destevez.net/2020/07/tianwen-1-telemetry-modulation-and-coding/.

Estévez, Daniel. GRCon 2020 workshop: Decoding interplanetary spacecraft, 2020b. URL https://www.gnuradio.org/grcon/grcon20/workshops/.

Kaminski, Heinz. Sternwarte Bochum beobachtet US-Apollo-Mondexperimente. *Neues v. Rohde und Schwarz*, (57):24–27, Oct/Nov 1972. ISSN 0548-3093.

Kaminski, Heinz. Data reception in the S-band - 1,7 and 2,3 GHZ - of NOAA- and ERTS- data - The 20-Metre-Parabolic Universal Antenna of Bochum. In *DGLR-Symposium Telemetrie-Messdatenerfassung, Echtzeitdatenreduzierung und -speicherung*, Munich, Jun 1976.

Kaplan, George H. The IAU resolutions on astronomical reference systems, time scales, and Earth rotation models. *United States Naval Observatory Circular*, (179), 2005.

Quantius, Dominik and Romberg, Oliver. DLR-AMSAT P5 Konzeptstudie zu einem Mond- und Marssatelliten in Kooperation mit AMSAT-DL - Executive Summary. Technical report, DLR- Institut für Raumfahrtsysteme, May 2010. URL https://elib.dlr.de/87078/.

Quantius, Dominik, Päsler, Hartmut, Braukhane, Andy, Gülzow, Peter, Bauer, Waldemar, Vollhardt, Achim, Schubert, Daniel, and Romberg, Oliver. Open source mission to the Moon. In *IAC 2010*, number IAC-10, September 2010. URL https://elib.dlr.de/66641/.

r00t.cz. Tianwen-1 Mars mission, 2020. URL https://www.r00t.cz/Sats/Tianwen1.

Ratti, Benoit, Thiry, Marc, and Lorenz, Mario. STEREO MISSION : CRYOGENIC LNA AND TURBOCODE. In *6th ESA International Workshop on Tracking, Telemetry and Command Systems for Space Applications*, Darmstadt, 2013.

Thinking Systems, Inc. GMAT, 2020. URL https://sourceforge.net/projects/gmat/.

Walls, Andy. GRCon 2017 talk: Symbol clock recovery and improved symbol synchronization blocks, 2017. URL https://www.youtube.com/watch?v=uMEfx_l5Oxk.

Wan, W.X., Wang, C., Li, C.L., and Wei, Y. China's first mission to Mars. *Nature Astronomy*, 4:721–721, 2020. doi: 10.1038/s41550-020-1148-6.

Wang, Yi, Li, Bo, Zhang, Jiang, Ling, Zongcheng, Qiao, Le, Chen, Shengbo, and Qu, Shaojie. The preliminary study of dust devil tracks in southern Utopia Planitia, landing area of Tianwen-1 mission. *Remote Sensing*, 13 (13), 2021a. doi: 10.3390/rs13132601.

Wang, Ying, Feng, Xuan, Zhou, Haoqiu, Dong, Zejun, Liang, Wenjing, Xue, Cewen, and Li, Xiaotian. Water ice detection research in Utopia Planitia based on simulation of Mars rover full-polarimetric subsurface penetrating radar. *Remote Sensing*, 13(14), 2021b. doi: 10.3390/rs13142685.

Wu, Bo, Dong, Jie, Wang, Yiran, Li, Zhaojin, Chen, Zeyu, Liu, Wai Chung, Zhu, Jiaming, Chen, Long, Li, Yuan, and Rao, Wei. Characterization of the Candidate Landing Region for Tianwen-1—China's First Mission to Mars. *Earth and Space Science*, 8(6), 2021. doi: 10.1029/2021EA001670.

Zou, Yongliao, Zhu, Yan, Bai, Yunfei, Wang, Lianguo, Jia, Yingzhuo, Shen, Weihua, Fan, Yu, Liu, Yang, Wang, Chi, Zhang, Aibing, Yu, Guobin, Dong, Jihong, Shu, Rong, He, Zhiping, Zhang, Tielong, Du, Aimin, Fan, Mingyi, Yang, Jianfeng, Zhou, Bin, Wang, Yi, and Peng, Yongqing. Scientific objectives and payloads of Tianwen-1, China's first Mars exploration mission. *Advances in Space Research*, 67(2):812–823, 2021. doi: 10.1016/j.asr.2020.11.005.